pISSN 2384-1095
eISSN 2384-1109

iMRI 2021;25:293-299

https://doi.org/10.13104/imri.2021.25.4.293

iMRI
Investigative Magnetic Resonance Imaging

Accelerating Magnetic Resonance Fingerprinting Using Hybrid Deep Learning and Iterative Reconstruction

Peng Cao[1*], Di Cui[1], Yanzhen Ming[1], Varut Vardhanabhuti[1], Elaine Lee[1], Edward Hui[2]

[1]Department of Diagnostic Radiology, The University of Hong Kong, Hong Kong, China
[2]Department of Rehabilitation Science, The Hong Kong Polytechnic University, Hong Kong, China

Purpose: To accelerate magnetic resonance fingerprinting (MRF) by developing a flexible deep learning reconstruction method.
Materials and Methods: Synthetic data were used to train a deep learning model. The trained model was then applied to MRF for different organs and diseases. Iterative reconstruction was performed outside the deep learning model, allowing a changeable encoding matrix, i.e., with flexibility of choice for image resolution, radiofrequency coil, k-space trajectory, and undersampling mask. *In vivo* experiments were performed on normal brain and prostate cancer volunteers to demonstrate the model performance and generalizability.
Results: In 400-dynamics brain MRF, direct nonuniform Fourier transform caused a slight increase of random fluctuations on the T2 map. These fluctuations were reduced with the proposed method. In prostate MRF, the proposed method suppressed fluctuations on both T1 and T2 maps.
Conclusion: The deep learning and iterative MRF reconstruction method described in this study was flexible with different acquisition settings such as radiofrequency coils. It is generalizable for different *in vivo* applications.

Keywords: Deep learning; Iterative reconstruction; MRF reconstruction; MRI reconstruction

Original Article

Received: February 1, 2021
Revised: May 26, 2021
Accepted: June 17, 2021

Correspondence to:
Peng Cao, M.D., Ph.D.
LG3, 5 Sassoon Road, Fok Fu Lam, Hong Kong, Hong Kong SAR, China.
Tel. +852-53761014
Fax. +852-25057866
E-mail: caopeng1@hku.hk

This is an Open Access article distributed under the terms of the Creative Commons Attribution Non-Commercial License (http://creativecommons.org/licenses/by-nc/4.0/) which permits unrestricted non-commercial use, distribution, and reproduction in any medium, provided the original work is properly cited.

Copyright © 2021 Korean Society of Magnetic Resonance in Medicine (KSMRM)

INTRODUCTION

Magnetic resonance fingerprinting (MRF) with a variable flip angle (VFA) scheme and a dictionary matching can provide time-efficient T1 and T2 quantifications (1). Clinically, MRF employing T1 and T2 (1) has been used to characterize brain tumors (2), breast cancer (3), and prostate cancer (4). MRF can acquire hundreds of dynamics with a high undersampling factor to characterize signal evolution and quantify T1 and T2 simultaneously (1). Considering that a certain number of dynamics (e.g., 700-1000) are needed for quantification, current MRF protocols generally took 7-10 seconds per slice. Acceleration methods are needed to speed up the MRF protocol.

MRF reconstruction is conventionally based on Fourier transform and dictionary matching (1). Like magnetic resonance imaging (MRI), MRF reconstruction can be modelled as the inversion of the encoding matrix that contains coil sensitivity, Fourier

transform, and k-space undersampling operators. The acceleration method such as compressed sensing and parallel imaging can be directly applied to MRF (5). In previous studies, a constraint for dictionary matching has been used, serving as a projection onto the feasible space for accurate T1 and T2 quantifications (6, 7).

Iterative reconstruction is conventionally used with compressed sensing, parallel imaging, and dictionary matching constraints (6, 7). These previous studies have used alternating direction method of multipliers (ADMM) to solve the problem of multiple constraints/regularizations (6, 7). The ADMM reconstruction with the constraint of dictionary matching has demonstrated the feasibility of accelerating MRF. Iterative reconstruction also allows a changeable encoding matrix with the flexibility of choice for image resolution, coil sensitivity profile, k-space trajectory, and undersampling mask.

Deep learning has recently been used as an alternative to regularized MRI reconstruction (8-10). It can improve reconstruction performance in some predetermined acquisition settings or pre-trained imaging tasks (8-10). However, it is not flexible for different under-sampling schemes in MRI acquisition. We have recently applied Bayesian inference to model MRI reconstruction using a statistical representation of an MRI database as a prior model (11). Our Bayesian MRI reconstruction uniquely supports changeable encoding matrix.

In conjunction with deep learning MRI, the deep learning MRF has also been extensively studied (12-17). In those studies, feed-forward networks that contained few fully connected layers or convolutional layers were used to perform T1 and T2 reconstructions (12-15) or quantifications (16-18). Feed-forward networks are usually fixed after model training. Thus, the encoding matrix is not changeable. A more recent study on a proximal network has echoed recent developments of deep learning MRI and defined regularization explicitly (19). However, abovementioned methods all require *in vivo* data for training the model, limiting their generalizability for different organs and diseases. Therefore, current deep learning MRF methods are limited by the fixed encoding matrix and the requirement of *in vivo* datasets for model training.

The objectives and innovations of this study are two-fold. Firstly, the proposed method used synthetic data to train the deep learning model and the resulted model could be applied to different organs and diseases. Secondly, iterative reconstruction was performed outside the deep learning model, allowing a changeable encoding matrix, i.e., with flexibility of choice for image resolution, radiofrequency coil, k-space trajectory, and undersampling mask. *In vivo* experiments were performed on normal brain and prostate cancer volunteers to demonstrate the model's performance and generalizability.

METHODS

MRF Acquisition, Post-Processing, and Dictionary Generation

MRF scan was performed on a Philips Achieva 3T system (Philips Healthcare, Best, The Netherlands). Details of the sequence were presented in our previous study (18). Briefly, fast imaging with steady state precession (FISP) MRF was performed with the following parameters: a "half-sine"-style variable flip angle, 1000 dynamics, spiral in-out readout, 2D acquisition, constant TE/TR = 6/12 ms, slice thickness = 5 mm, matrix size = 256 × 256, number of total spiral interleaves = 48, and golden angle rotation scheme.

The local institutional research ethics committee approved *in vivo* experiments. For brain MRF, a normal volunteer was scanned using the MRF sequence. Only one slice was acquired with a scan time of 12 seconds. For prostate MRF, a prostate cancer patient was scanned with the same MRF protocol and eight slices were acquired with a scan time of 1 minute and 36 seconds.

ESPIRiT coil sensitivity (20) was then calculated based on the sum for all dynamics. The k-space data were first compressed into four singular value components. Details of k-space compression will be presented in another study. Non-uniform Fourier transform was performed in a python and tensorflow environment (https://www.tensorflow.org/) using an open-source package (https://github.com/zaccharieramzi/tfkbnufft). Reconstruction algorithms were developed using the "eager mode" in tensorflow software.

Iteration of reconstruction was implemented in a conventional regularized optimization method, i.e., proximal gradient descent. The deep learning model served as the proximal operator that could be inserted into regularized optimization methods. This approach was inspired by a recent paper on proximal gradient network (19). Our study used synthetic data to train the deep learning model outside the iterative reconstruction algorithm. The proposed method was generalizable for different organs and encoding matrices.

Regularization Using a Deep Learning Model

The cost function for deep learning-based MRF reconstruction is given as follows:

$$L_R(x) = ||PFSx-y||_2^2 + R(x) \quad \text{Eq. 1}$$

where x is image series, y is k-space data, R is deep learning-based regularization, S is coil sensitivity profile, F is non-uniform Fourier transform, and P is the undersampling mask. Minimizing the L_R can allow reconstruction of MRF image series. Noted that x, y, and P are all compressed to four singular values. For simplicity, we can rewrite the encoding matrix as $A = PFS$.

The deep learning model serves as the proximity operator for regularization R. It is written as follows:

$$Prox_R(x) = argmin_x ||x-x_0||_2^2 + R(x) \quad \text{Eq. 2}$$

Where x_0 is the input for the proximity operator, i.e., the input for the deep learning model. In intuitively, the deep learning could output the solution x that is near the input x_0 in a norm-2 distance sense.

Proximal Gradient Descent

The proximal gradient descent for solving Eqs. 1 and 2 is given as follows:

$$g(x^k) = ||Ax^k-y||_2^2$$

$$x^{k+1} = Prox_R(x^k - t\,\nabla g(x^k)),\ k = 1, 2, 3,... \quad \text{Eq. 3}$$

where g is the fidelity term in Eq. 1 and $Prox_R$ is the deep learning model, leading to the regularization term in Eq. 1. The gradient of fidelity term, i.e., ∇g, is given as follows:

$$\nabla g(x) = A^H(Ax - y) \quad \text{Eq. 4}$$

In this study, Eqs. 3 and 4 were solved outside the deep learning model so that the encoding matrix, $A = PFS$, was changeable for different acquisition settings.

Deep Learning Implementation

The deep learning structure was inspired by the encoder-decoder structure in a previous study (19), mimicking dictionary matching and back projection processes as shown in Figure 1. On the encoder side, the input was the synthetic/*in vivo* MRF image with artifacts. The output of the encoder was T1, T2, and proton density (PD) estimates. The encoder was a multi-layer perceptron (MLP) with four fully connected layers implemented with 1 × 1 convolution layers. The width of fully connected layers was 512 and the activation was RELU. This structure was used in our previous study for T1 and T2 quantifications (18). Two 1 × 1 convolutional layers and two 2 × 2 convolution layers were used to recreate artifact-free image from T1, T2, and proton density values on the decoder side. Third layer features on the encoder side were used to gate (via multiplication) decoder side features as shown in Figure 1. Such by-passing and gating allowed information to flow from the encoder to the decoder.

Synthetic Data Formation and Model Training

Synthetic data were simulated using dictionary elements filled in some artificial shapes in the image domain as shown in Figure 2. Artifact simulation was based on the method used in our previous study (18). Briefly, artifacts were randomly picked dictionary elements times random weights. When training the network, input images had artifacts added. Meanwhile, output images had no artifacts

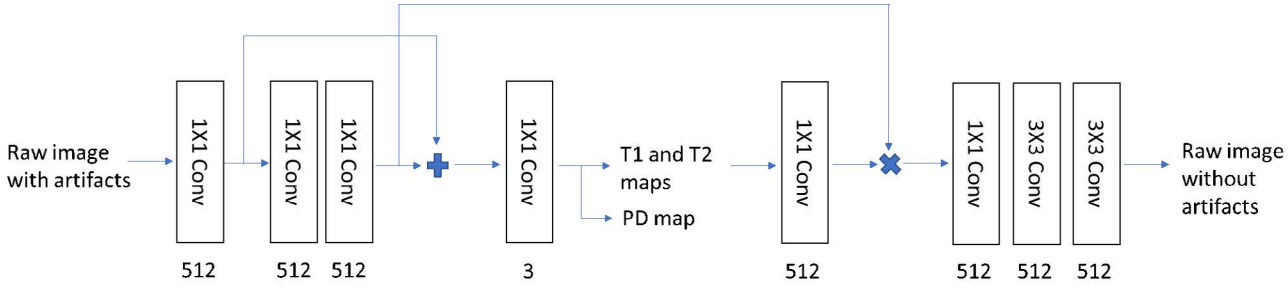

Fig. 1. Diagram showing the deep learning model used in this study. The model contained eight convolution layers. The first four 1 × 1 convolution layers served as the encoder that converted raw images into T1, T2, and proton density parameters. The other four convolution layers projected T1 and T2 parameters to the original raw image space. A residual connection was used on the network's left side to improve training efficiency and convergence. A gate structure, i.e., multiplication, was used on the right side to combine the features from the right side with those from the decoder layer.

as shown in Figure 2. We defined two loss terms: MRF loss for T1, T2, and PD quantification (i.e., *Loss_MRF*) and image reconstruction loss for artifact reduction on input images (i.e., *Loss_recon*). We used the mean square error function (i.e., tensorflow 'mean_squared_error' function) for training these two loss terms. Finally, the deep learning model learned to remove artifacts and project the image onto the nearest elements in a dictionary, i.e., the proximity operator for regularization. Deep learning model training was performed in tensorflow software on a laptop computer with one RTX 2080 NIVIDIA graphic card. The reconstruction was performed on a workstation equipped with a 50-core CPU, 512 G RAM, and a P6000 NIVIDA graphic card.

RESULTS

In vivo Brain MRF

The proposed method was first evaluated with brain MRF data as shown in Figure 3. Brain MRF data had a relatively high signal to noise ratio and allowed reliable estimation of T1 and T2 maps even with only 400 dynamics used in reconstruction. Meanwhile, direct NUFFT caused a slight increase in random fluctuation on the T2 map, which was reduced by the proposed method.

In vivo Prostate MRF

The proposed method was also applied to prostate MRF data as shown in Figure 4. The NUFFT on both 1000 and

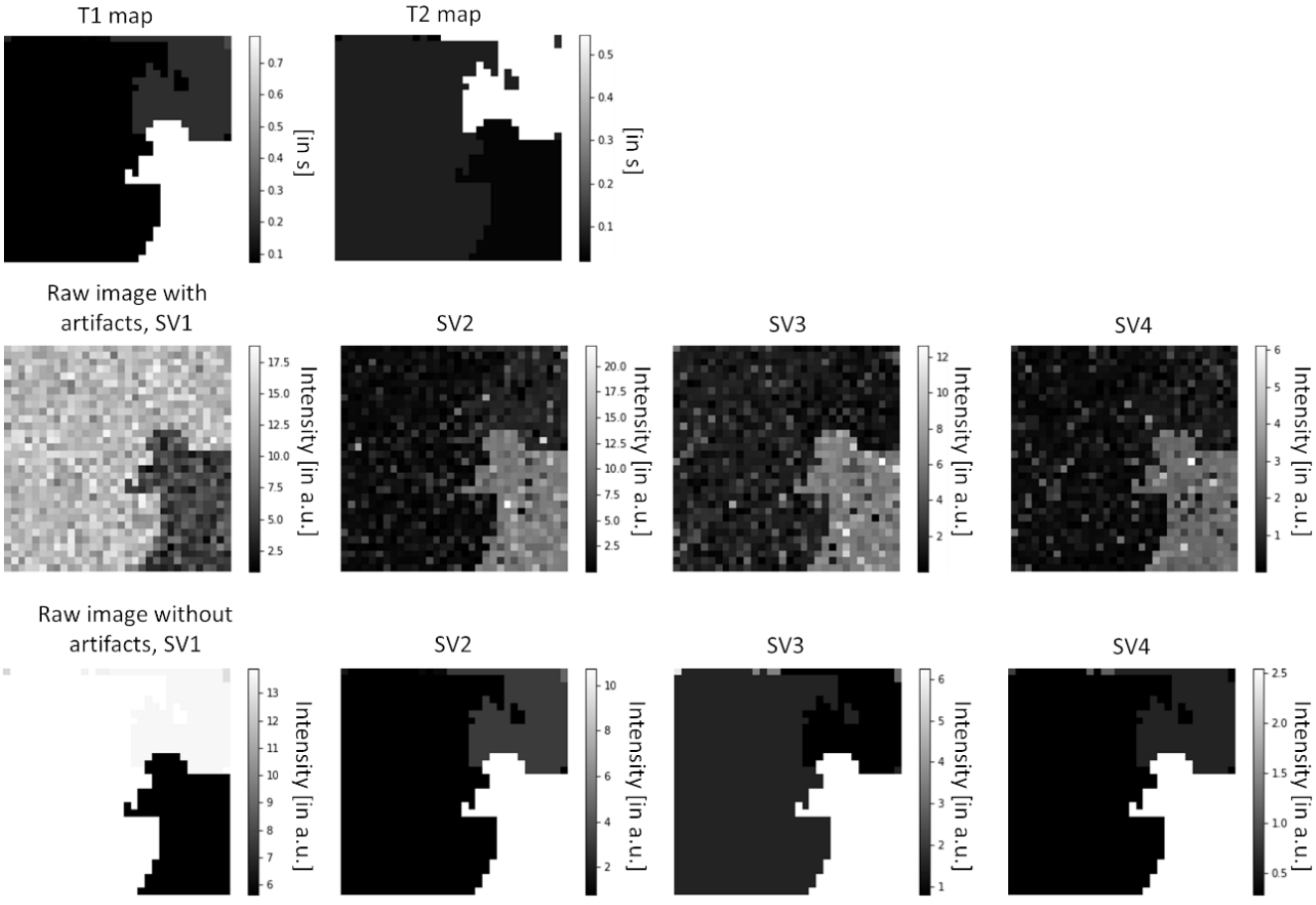

Fig. 2. Synthetic MRF images with/without artifacts were used to train the deep model. (First row) T1 and T2 were randomly placed in artificial shapes in a 32 × 32 matrix. T1 and T2 labels were from a dictionary that was simulated using extended phase graph. (Second row) Raw images with singular value decomposion compression. Four singular value components (SVs) were plotted. Raw images with artifacts served as input of the deep learning model. (Third row) Four SVs for raw image without artifacts. Artifact-free images were considered as the output of the deep learning model in this study. The deep learning model was trained to remove artifacts in images.

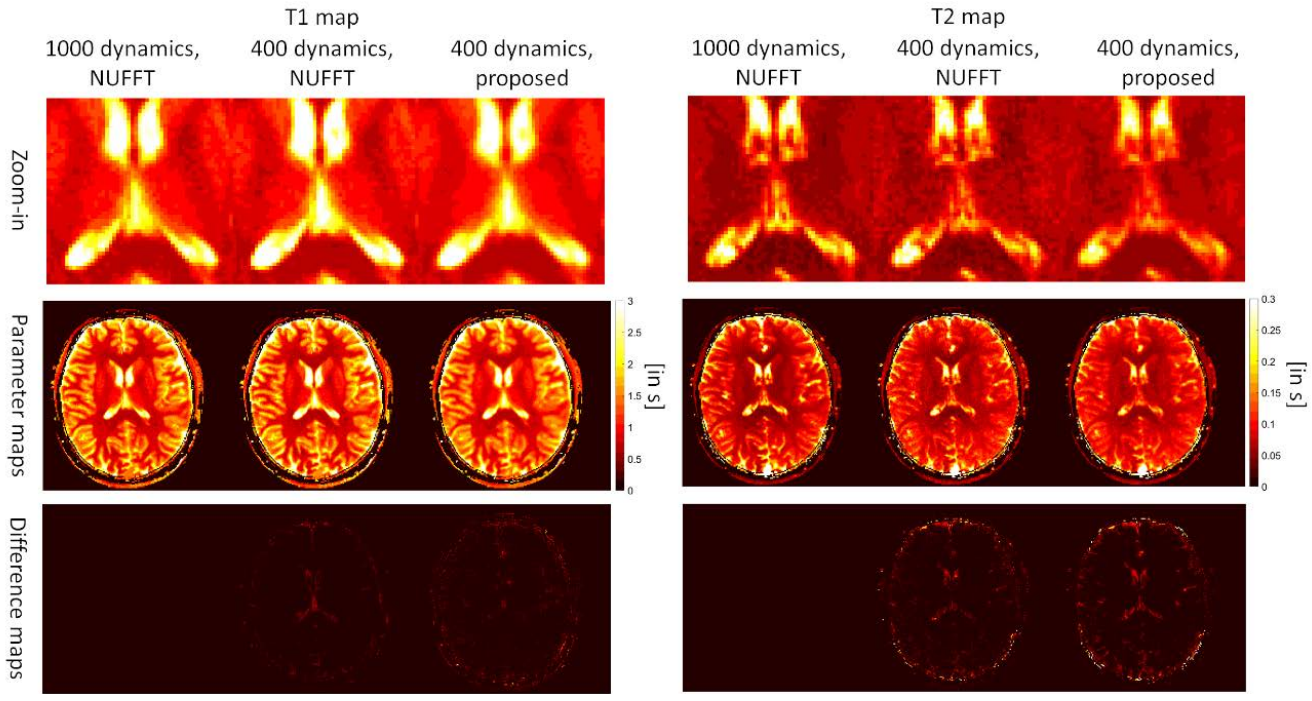

Fig. 3. The proposed deep learning approach was applied to brain MRF data. Zoom-in views were from the center area. Direct NUFFT on 400 dynamic data showed slightly increased random fluctuations in T2 maps. The proposed method effectively reduced such random fluctuations in T2 maps, showing a strong de-noising effect on T1 and T2 maps. Difference maps measured discrepancies between 1000-dynamic NUFFT results and 400-dynamic NUFFT or proposed methods.

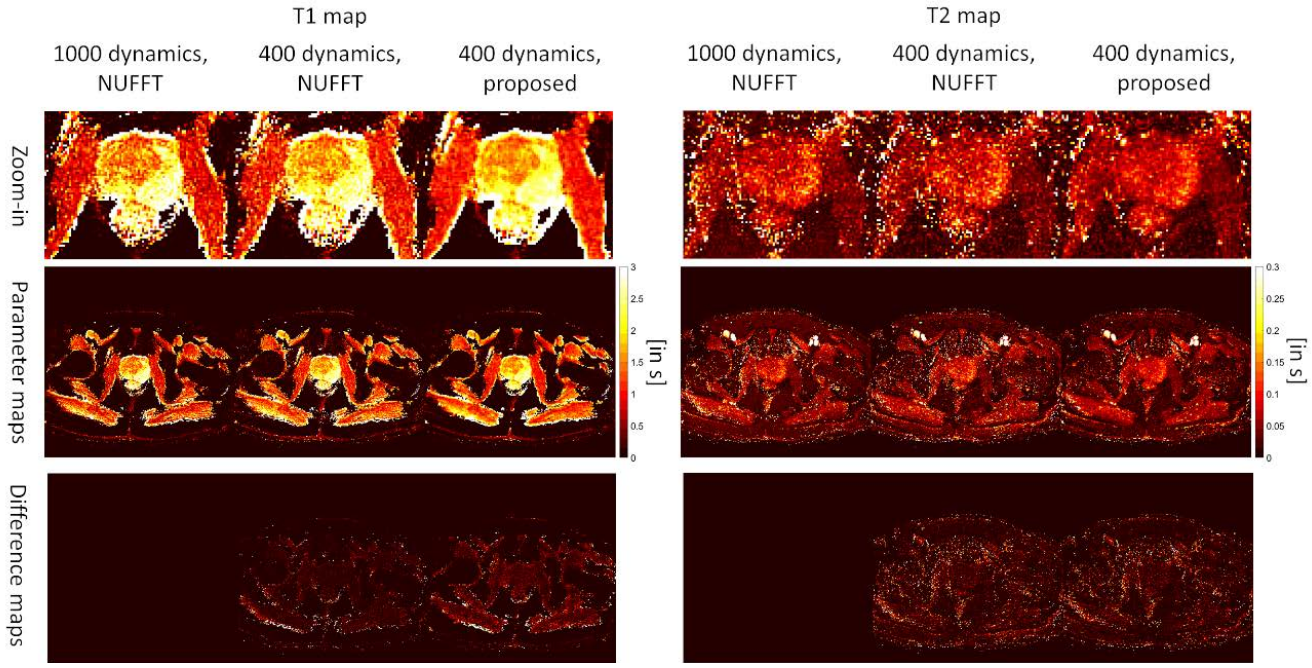

Fig. 4. The proposed deep learning approach was applied to prostate MRF data. Zoom-in views were from the center area. Direct NUFFT on 400 dynamic data showed increased random fluctuations in both T1 and T2 maps. The proposed method effectively reduced random fluctuations. The difference maps measured discrepancies between 1000-dynamic NUFFT results and 400-dynamic NUFFT results or proposed methods.

400 dynamics datasets had relatively high fluctuations. The proposed method suppressed these fluctuations in both T1 and T2 maps. Results were consistent with the observation in brain MRF. NUFFT results for 1000 dynamic datasets were used as reference. The slight increase in difference between the proposed method and reference reflected a strong denoising effect of the proposed method on parameter maps. In addition, Figure 5 shows the algorithm rapidly converged to the optimal solution in 25 iterations. The reconstruction time was 86 seconds per slice.

DISCUSSION

As *in vivo* data are typically used in training conventional deep learning MRF models, their generalizability could be limited to specific organs or diseases involved in the training process. The proposed method used synthetic data to train the deep learning model. The trained deep learning model could be applied to different organs. For example, a trained model was used for both brain and prostate in this study, showing that a single model could be applied to MRF for two organs. Prostate scan and brain scan had different coil sensitivity profiles, causing varied encoding matrix in reconstructions. The proposed method could support reconstructions of two scan protocols using one deep learning model. Therefore, application of the proposed method was just like conventional parallel imaging and compressed sensing approaches. Such improvement greatly simplified the experimental design, allowing one deep learning model to be generalizable for different applications *in vivo*.

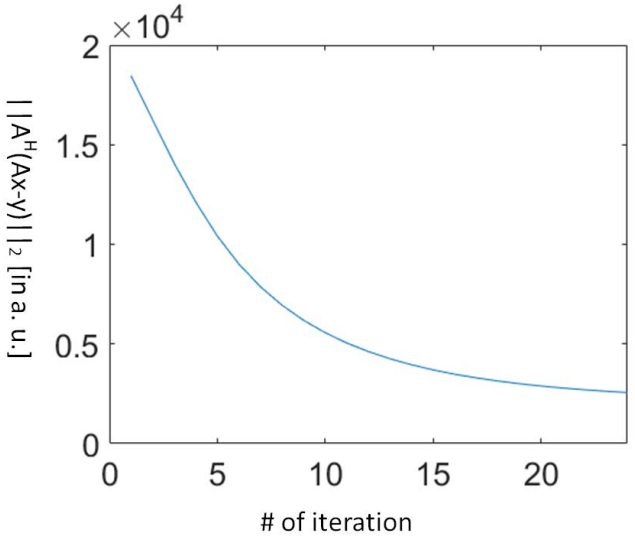

Fig. 5. Converge curve of the proximal gradient descent in brain MRF experiment. The plot shows gradient of fidelity term in Eq. 1, which is decreased with increasing number of iteration. The algorithm rapidly converged to optimal solution.

The method also supported different MRI encoding settings such as image resolutions, undersampling masks, and radiofrequency coils. The encoding matrix was used in the fidelity term, which was outside and independent of the deep learning model. The encoding matrix contained coil sensitivity, trajectory, and undersampling mask. It was changeable during reconstruction, i.e., the deep learning model could be applied to different experiments without needing re-training of the model. In this study, brain and prostate MRF datasets were acquired with totally different brain and dorsal coils. However, they were reconstructed with the same deep learning model and algorithm. The same deep learning model could be used in all MRF reconstructions, demonstrating its great flexibility and generalizability in clinical applications. Therefore, the deep learning model could perform artifact removal and support changeable MRF acquisition settings.

In summary, we used an MLP-encoder to perform pixel-wise encoding. We empirically found that the MLP maintained spatial resolution. Meanwhile, we used kernel size of convolutional layers on the decoder side to adjust denoising vs. spatial smoothing effect. The MLP might not be the only way for MRF. Generally, fully convolutional networks should be supported by the proposed architecture. In addition, we used the same weight for all iterations. This ensured a small network that was end-to-end trainable. The number of iterations for the proposed network was also changeable during reconstruction.

In conclusion, we demonstrated a hybrid iterative MRF reconstruction method that was flexible with different acquisition settings, such as radiofrequency coils and generalizable for *in vivo* applications.

Acknowledgments

The work was partly funded by Hong Kong RGC General Research Fund (17117018) and Hong Kong Health and Medical Research Fund (07182706 and 06172916).

REFERENCES

1. Ma D, Gulani V, Seiberlich N, et al. Magnetic resonance

fingerprinting. Nature 2013;495:187-192
2. Badve C, Yu A, Dastmalchian S, et al. MR fingerprinting of adult brain tumors: initial experience. AJNR Am J Neuroradiol 2017;38:492-499
3. Chen Y, Panda A, Pahwa S, et al. Three-dimensional MR fingerprinting for quantitative breast imaging. Radiology 2019;290:33-40
4. Yu AC, Badve C, Ponsky LE, et al. Development of a combined MR fingerprinting and diffusion examination for prostate cancer. Radiology 2017;283:729-738
5. Liao C, Bilgic B, Manhard MK, et al. 3D MR fingerprinting with accelerated stack-of-spirals and hybrid sliding-window and GRAPPA reconstruction. Neuroimage 2017;162:13-22
6. Asslander J, Cloos MA, Knoll F, Sodickson DK, Hennig J, Lattanzi R. Low rank alternating direction method of multipliers reconstruction for MR fingerprinting. Magn Reson Med 2018;79:83-96
7. Cline CC, Chen X, Mailhe B, et al. AIR-MRF: accelerated iterative reconstruction for magnetic resonance fingerprinting. Magn Reson Imaging 2017;41:29-40
8. Yang Y, Xu Z, Song D. Missing value imputation for microRNA expression data by using a GO-based similarity measure. BMC Bioinformatics 2016;17 Suppl 1:10
9. Schlemper J, Caballero J, Hajnal JV, Price AN, Rueckert D. A deep cascade of convolutional neural networks for dynamic MR image reconstruction. IEEE Trans Med Imaging 2018;37:491-503
10. Aggarwal HK, Mani MP, Jacob M. MoDL: model-based deep learning architecture for inverse problems. IEEE Trans Med Imaging 2019;38:394-405
11. Luo G, Zhao N, Jiang W, Hui ES, Cao P. MRI reconstruction using deep Bayesian estimation. Magn Reson Med 2020;84:2246-2261
12. Virtue P, Yu SX, Lustig M. Better than real: complex-valued neural nets for MRI fingerprinting. 2017 IEEE International Conference on Image Processing (ICIP), 2017:3953-3957
13. Cohen O, Zhu B, Rosen MS. MR fingerprinting Deep RecOnstruction NEtwork (DRONE). Magn Reson Med 2018;80:885-894
14. Chen Y, Fang Z, Hung SC, Chang WT, Shen D, Lin W. High-resolution 3D MR fingerprinting using parallel imaging and deep learning. Neuroimage 2020;206:116329
15. Barbieri M, Brizi L, Giampieri E, et al. Circumventing the curse of dimensionality in magnetic resonance fingerprinting through a deep learning approach. arXiv preprint arXiv:1811.11477, 2018
16. Fang Z, Chen Y, Lin W, Shen D. Quantification of relaxation times in MR fingerprinting using deep learning. Proc Int Soc Magn Reson Med Sci Meet Exhib Int Soc Magn Reson Med Sci Meet Exhib 2017;25
17. Fang Z, Chen Y, Hung SC, Zhang X, Lin W, Shen D. Submillimeter MR fingerprinting using deep learning-based tissue quantification. Magn Reson Med 2020;84:579-591
18. Cao P, Cui D, Vardhanabhuti V, Hui ES. Development of fast deep learning quantification for magnetic resonance fingerprinting in vivo. Magn Reson Imaging 2020;70:81-90
19. Chen D, Davies ME, Golbabaee M. Compressive MR fingerprinting reconstruction with neural proximal gradient iterations. In: Martel AL, Abolmaesumi P, Stoyanov D, eds. Lecture notes in computer science (including subseries lecture notes in artificial intelligence and lecture notes in bioinformatics). Cham, Swizerland: Springer Sience and Buiness Media Deutschland GmbH, 2020:13-22
20. Uecker M, Lai P, Murphy MJ, et al. ESPIRiT--an eigenvalue approach to autocalibrating parallel MRI: where SENSE meets GRAPPA. Magn Reson Med 2014;71:990-1001